Article citation info:
Zhou L, Li K, Sun T. Studies on the flame structure and drag of a combusting droplet group. Combustion Engines. 2023;193(2):3-8. https://doi.org/10.19206/CE-160506

Lixing ZHOU
Ke LI
Ting SUN

Combustion Engines
Polish Scientific Society of Combustion Engines

Studies on the flame structure and drag of a combusting droplet group

ARTICLE INFO

Received: 16 December 2022
Revised: 26 January 2023
Accepted: 3 February 2023
Available online: 13 February 2023

Droplet combustion has been studied by experiments and numerical simulation for many years, and most of studies were done about single droplets. As for droplet groups, some theoretical and experimental studies were reported, but less of numerical studies. One of the important characteristics is the drag of combusting droplets, which is closely related to flame structure, and is a sub-model in numerical simulation of spray combustion. There are contradictory research results for the drag of combusting droplets. In the present paper, large-eddy simulation (LES) is used to study the flame structure and drag of a combusting ethanol-droplet group. The results show that there are three combustion modes: fully-enveloped flame, partially-enveloped flame and wake flame in a droplet group, leading to the change of the drag with inlet velocities. It is found that the drag of droplets in the group is much smaller than that of a non-combusting particle in isothermal flows.

Key words: *droplet-group combustion; large-eddy-simulation; flame structure; drag force*

1. Introduction

Spray combustion is widely encountered in various engines [1–3]. It was studied by large-eddy simulation [4, 5], where droplets were taken as volume-less point-source particles. Droplet combustion is an important part of spray combustion. The droplet combustion has been studied both experimentally and analytically for many decades since the middle's years of the last century [6–9]. The experiments were done for suspended droplets, falling droplets and flying droplets of different fuels. The so-called d^2-law was examined and the "evaporation constant" $K = d(d_p^2/dt)$ under different gas relative velocities, gas temperatures and pressures were studied. In analytical studies, most of them are based on simplified 1-D "spherical stagnant-film" models. Even now, the sub-models for spray combustion in modern CFD software are still based on these models. These simplified studies cannot give the detailed structures of droplet flames. In recent years, more detailed theoretical, experimental and numerical studies of droplet combustion were reported. Awasthi et al. [10] simulated the effect of ambient temperature and initial droplet size on the combustion of a heptane droplet. The focus was paid on the heptane-droplet ignition delay and the comparison between the heptane and methanol droplets in flame location and evaporation rates. Kitano et al. [11] simulated single and multiple-droplet combustion, but used a given evaporation model to study the effect of ambient pressure and gas temperature on droplet evaporation. No information on the detailed gas flow, species concentration and gas temperature distributions surrounding the droplets were reported. Zhao et al. [12] simulated the effect of gas temperature on droplet combustion, only the effect of gas temperature on the droplet evaporation rate was reported and the comparison was given with the numerical results of other investigators. Chiu et al. [13, 14] reported an analytical model of droplet-group combustion. Segawa et al. [15] studied experimentally the ignition and early combustion behavior of 49 droplets under microgravity condition. Mikami et al. [16, 17] reported the droplet interactions in flame spreading characteristics of 100 n-decane droplets under micro-gravity conditions. Manish and Sahu [18] used PIV (particle imaging velocimetry) to measure the group combustion of droplet clusters in spray flames.

Regarding to droplet combustion characteristics, the drag force of evaporating/combusting droplets is an important sub-model in spray combustion modeling. Different research results were reported. The measurement results reported by Eisenklam et al. [19] are that evaporation reduces the droplet drag. Yuen et al. [20] did experimental studies, and Renksizbulut and Yuen [21] did analytical studies of different evaporating droplets; the conclusion is that evaporation does not affect the droplet drag. Makino and Fukada [22] measured the velocity of a falling combusting sodium droplet. The results show that combustion increases the droplet drag. Sugimoto [23] measured the velocity of a combusting methanol droplet; the results are that combustion reduces the droplet drag.

In general, the flow and flame structures surrounding a combusting droplet-group are unclear and the drag of combusting droplet group has not been reported. In this paper, large-eddy simulation (LES) is used to study a combusting ethanol-droplet group. The obtained flame structures and drag force are reported. The results will help to improve the drag model in numerical simulation of spray combustion in engines

2. Controlling equations and closure models for LES of a droplet-group combustion

To study the detailed flow and flame structures surrounding ethanol droplet group, the filtered governing equations for 3-D LES are given as

$$\frac{\partial \rho}{\partial t} + \frac{\partial \rho}{\partial t}(\rho \bar{u}_i) = 0 \tag{1}$$

$$\frac{\partial}{\partial t}(\rho \bar{u}_i) + \frac{\partial}{\partial x_j}(\rho \bar{u}_i \bar{u}_j) = \frac{\partial}{\partial x_j}\left(\mu \frac{\partial \bar{u}_i}{\partial x_j}\right) - \frac{\partial \bar{p}}{\partial x_i} - \frac{\partial \tau^{sgs}_{ij}}{\partial x_j} \tag{2}$$

$$\frac{\partial \rho \overline{Y_s}}{\partial t} + \frac{\partial}{\partial x_j}(\rho \bar{u}_j \overline{Y_s}) = \frac{\partial}{\partial x_j}\left(\frac{\mu}{S_c}\frac{\partial \overline{Y_s}}{\partial x_j}\right) - \overline{w_s} - w_{sgs} - \frac{\partial g_{jsgs}}{\partial x_j} \tag{3}$$

$$\frac{\partial \rho \bar{h}}{\partial t} + \frac{\partial}{\partial x_j}\left(\rho \bar{h} \bar{u}_j\right) = \frac{\partial}{\partial x_j}\left(\frac{\mu}{Pr}\frac{\partial \bar{h}}{\partial x_j}\right) - \frac{\partial q_{jsgs}}{\partial x_j} \quad (4)$$

The sub-grid-scale (SGS) stress was closed by the dynamic eddy-viscosity model [24]

$$\tau_{ij}^{sgs} = 2\rho C_s \bar{\Delta}^2 |\bar{S}| \overline{S_{ij}}$$

$$C_s = -\frac{1}{2}\frac{\langle L_{ij}\bar{S}_{ij}\rangle}{\hat{\Delta}^2\langle|\hat{\bar{S}}|\hat{\bar{S}}_{ij}\bar{S}_{ij}\rangle - \bar{\Delta}^2\langle|\hat{\bar{S}}|\hat{\bar{S}}_{ij}\bar{S}_{ij}\rangle} \quad (5)$$

where $L_{ij} = \bar{u}_i\bar{u}_j - \tilde{\bar{u}}_i\tilde{\bar{u}}_{ij}$, $\tilde{\Delta} = 2\bar{\Delta}$, $\bar{\Delta}$ is the filter size/grid size, and

$$A = \frac{1}{2}\left(\frac{\partial \tilde{\bar{u}}_i}{\partial x_j} + \frac{\partial \tilde{\bar{u}}_j}{\partial x_i}\right);\ \left|\hat{\bar{S}}\right| = \sqrt{2\hat{\bar{S}}_{ij}\hat{\bar{S}}_{ij}}$$

The SGS mass and heat fluxes are closed by gradient modeling

$$g_{jsgs} = \rho\left(u_j Y_s - \bar{u}_j \bar{Y}_s\right) = \frac{\mu_t}{\sigma_Y}\frac{\partial \bar{Y}_s}{\partial x_j} \quad (6)$$

$$q_j{}^{sgs} = \rho\left(u_j T - \bar{u}_j \bar{T}\right) = \frac{\mu_t}{\sigma_T}\frac{\partial \bar{T}}{\partial x_j} \quad (7)$$

The sub-grid scale reaction rate is closed by the second-order moment combustion model [25]

$$w_{sgs} = \bar{w}_s\left(\frac{\overline{Y_1'Y_2'}}{\bar{Y}_1\bar{Y}_2} + \frac{\overline{K'Y_1'}}{\bar{K}\bar{Y}_1} + \frac{\overline{K'Y_2'}}{\bar{K}\bar{Y}_2}\right)$$

$$\overline{\phi\varphi} = \frac{c\mu_t\left(\frac{\partial \Phi}{\partial x_j}\right)\left(\frac{\partial \Psi}{\partial x_j}\right)}{\rho} \Big/ \left(\frac{a}{\tau_T} + \frac{1-a}{\tau_c}\right) \quad (8)$$

where Φ, Ψ, ϕ and φ denote the filtered and sub-grid-scale fluctuation values of Y_1, Y_2 and K respectively.

$$\tau_T = 1/|\bar{S}|;\ \tau_c = \left[B\rho\left(\bar{Y}_{O_2} + \beta\bar{Y}_{CH_4}\right)\exp\left(-\frac{E}{R\bar{T}}\right)\right]^{-1}$$

For ethanol-oxygen reaction mechanism, a global single-step reaction is used

$$2C_2H_5OH + 6O_2 \rightarrow 4CO_2 + 6H_2O \quad (9)$$

The Arrhenius expression of the single-step global reaction kinetics for the reaction rate is

$$w_s = 8.345 \times 10^9 \rho^2 Y_{fu} Y_{ox} \exp[-1.26 \times 10^8/(RT)] \quad (10)$$

with boundary conditions at the droplet surface, accounting for the Stefan flux

$$\lambda_w\left(\frac{dT}{dr}\right)_w = \rho_w \nu_w q_e =$$

$$= \frac{G}{4\pi r_w^2} q_e - D_w \rho_w \left(\frac{dY}{dr}\right)_w + Y_s \rho_w \nu_w = \alpha \rho_w \nu_w$$

$$\Sigma Y_s = \Sigma Y_F + \Sigma Y_{ox} + \Sigma Y_{pr} + \Sigma Y_{in} = 1$$

where, s = F(fuel), $\alpha = 1$, $s \neq F$, $\alpha = 0$. α is a notation for different species. For obtaining the fuel vapor concentration, the fuel vapor partial pressure should be obtained by using the Antoine equation.

3. Computation domain and solution procedure

The computation domain is shown in Fig. 1. The sizes and position of simulated droplets are shown in Fig. 2 and Table 1. The grid sizes in x, y, and z directions are 10–300 μm; the time step was taken as 0.000001 s; and the grid number is about 1400000.

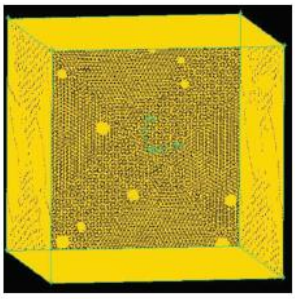

Fig. 1. Computation domain

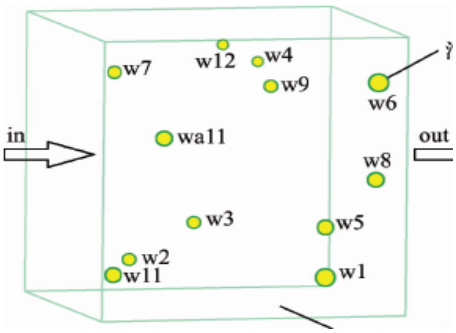

Fig. 2. Droplet sizes and position

The PISO algorithm was used for p–v corrections; the second-order implicit difference scheme was taken for the time-dependent term, the second-order upwind difference scheme was taken for the convection term, and the central difference scheme was taken for the diffusion term. For the gas boundary conditions, a uniform gas inlet velocity was taken. The boundary condition at the exit was based on a fully developed flow assumption, where the gradients for all flow variables in the axial direction were set to be zero.

Table1. Droplet sizes and position

Group No./ Droplet size [μm]		Droplet position		
		x [μm]	y [μm]	z [μm]
w1	34.3	301.5	–433.7	515.1
w2	21.5	–293.9	–420.8	–180.0
w3	27.3	7.1	–291.0	–364.1
w4	17.1	238.9	408.9	–298.7
w5	29.2	469.1	–294.9	–139.3
w6	36.4	551.1	377.1	334.1
w7	23	–507.9	451.4	394.6
w8	27.9	496.1	–17.5	520.8
w9	20.3	158.8	360.3	214.5
w10	32.8	–483.0	–429.7	309.3
w11	19.4	56.3	498.9	–129.3
w12	30.6	–257.0	137.0	195.5

4. Simulation results

4.1. Instantaneous flame structures

Figure 3 shows three combustion modes of the droplet group. There are fully-enveloped flame, partially-enveloped flame and wake flame under different gas relative velocity, similar to the numerical results of a single droplet [26], and the PLIF measurement results obtained by Mercier et al.

[27]. However, in case of the droplet group, different combustion modes may exist in the same region, since there are different droplet sizes in a computation domain. Since the Stefan flow surrounding the droplets in the azimuthal direction is non-uniform, which will cause the change of drag with the inlet velocity.

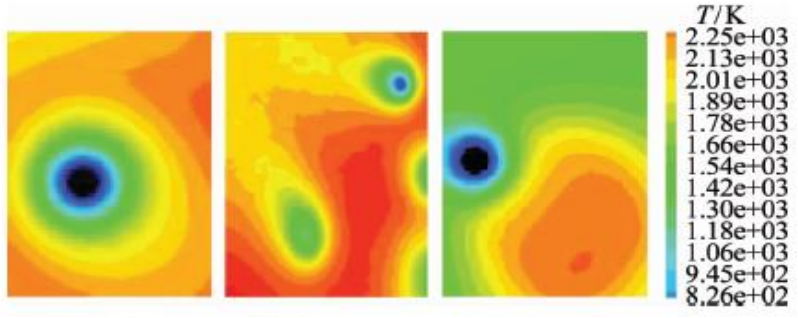

(a) 1 m/s (b) 4 m/s (c) 10 m/s

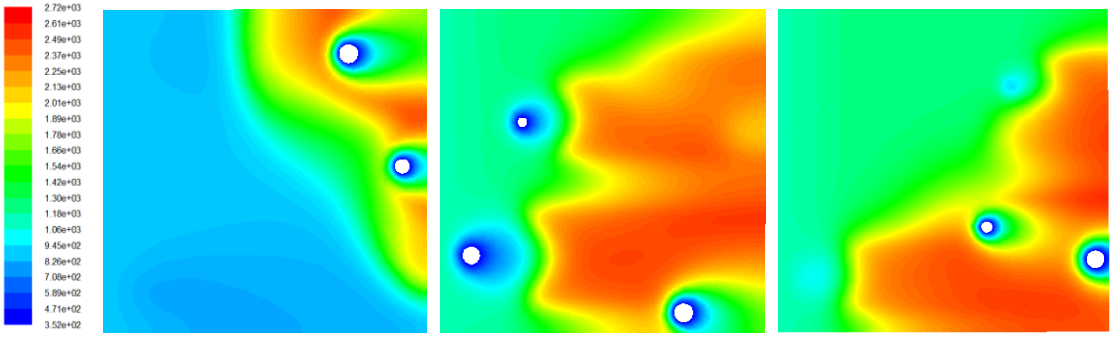

(d) (gas velocity 4m/s, gas temperature 1200 K)

Fig. 3. Three combustion modes of multiple droplets

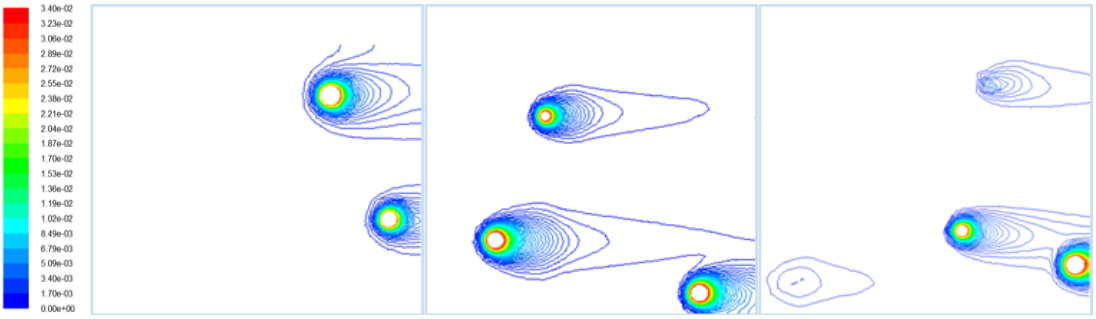

Fig. 4. Molar fraction of ethanol-vapor concentration

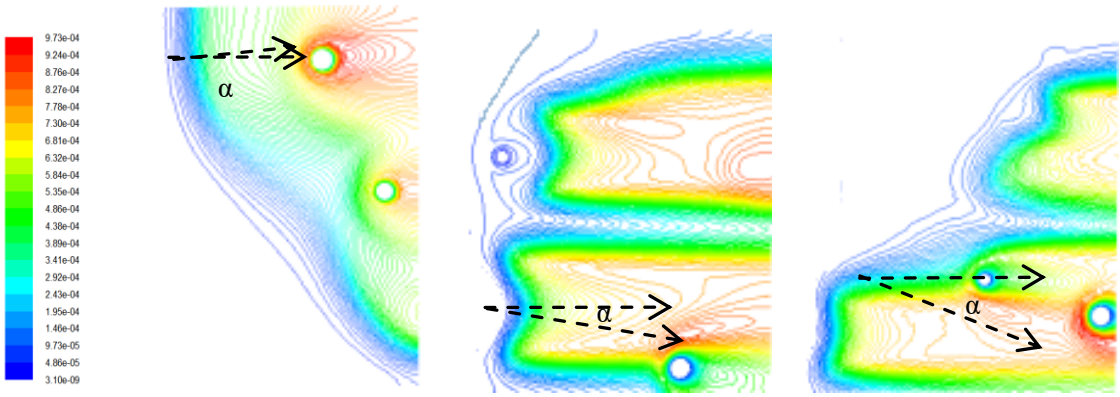

Fig. 5. Molar fraction of H_2O concentration

Figures 4 and 5 show the predicted molar fractions of ethanol-vapor and H_2O surrounding the droplet group respectively. The distribution of ethanol-vapor concentration is axis-symmetrical, but the reaction zones are somewhat declined with an angle of α due the interaction between droplets. Figures 6 and 7 are velocity vectors and streamlines surrounding the combusting droplet group respectively. Obviously, velocities ahead of droplets are larger than those behind droplets due to the Stefan flow, leading to the change of drag. The similar phenomenon was observed in the velocity vectors surrounding a single droplet [26]. The streamlines are distorted due to the interaction between droplets.

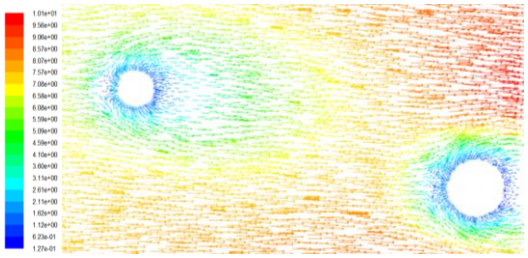

Fig. 6. Velocity vectors surrounding combusting droplets

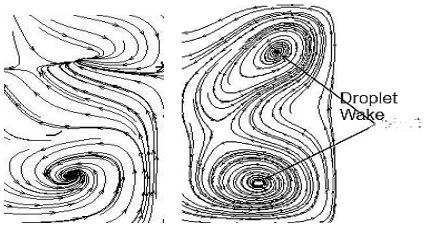

Fig. 7. Streamlines surrounding combusting droplets

Figure 8 gives the vorticity maps surrounding a droplet group and a single droplet. The vortex shedding in a droplet inside the group is weaker than that in a single droplet owing to droplet-droplet interactions.

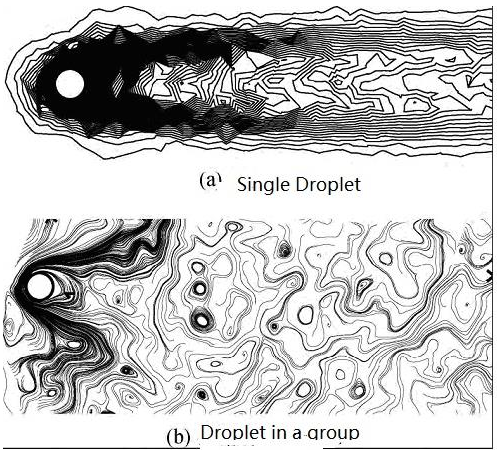

Fig. 8. Vorticity maps surrounding a droplet group

4.2. Statistics of the combusting droplet drag

The statistics gives the comparison between the widely-used Wallis-Kliachko formula of the drag for non-combusting particles in isothermal flows, modified droplet drag accounting the effect of the Stefan Flow given by the 1-D model [28] and the LES results for a single combusting droplet, as shown in Table 2. The Wallis-Kliachko formula [28] gives

$$C_{D0} = \begin{cases} \dfrac{24}{Re_p}\left(1 + Re_p^{2/3}/6\right) & Re_p < 1000 \\ 0.44 & Re_p \geq 1000 \end{cases}$$

$$Re_p = \frac{\rho_f d_p \left|\vec{U}_f - \vec{U}_p\right|}{\mu_f}$$

The modified formula in the 1-D stagnant-film theory [28] gives

$$C_D = C_{D0}\ln(1+b)/B;\ B = c_p(T_g - T_b)/L$$

where B is the transfer number, related to the boiling point and latent heat of the liquid.

Obviously, the drag coefficient of combusting droplet is much smaller than that of non-combusting particles in isothermal flows. The physical explanations may be the injection effect of non-uniform Stefan flow surrounding the combusting droplet and the effect of cold droplet-surface temperature on the reduction of friction force due to the reduction of gas viscosity.

Table 2. Drag coefficients for a single combusting droplet (T_g = 1200 K)

V_{rel} [m/s]	C_{D0} (Wallis-Kliachko Formula)	C_D (LES)	C_{D0} × × ln (1+B)/B
0.2	3.950	1.100	2.370
1.0	1.960	0.344	1.176
4.0	0.963	0.235	0.576

The drag coefficient of a droplet in its group is still smaller than that of a single droplet, as shown in Table 3.

Table 3. Drag coefficients for a droplet in its group

V_{rel} [m/s]	C_D (Wallis-Kliachko)	C_D (Single droplet)	C_D (Droplet in a group)
1	1.960	0.344	0.297
4	0.963	0.235	0.144

Figure 9 gives the drag coefficient of the single combusting droplet vs droplet Reynolds number, reported in [26]. It is seen that as the droplet Reynolds number increases to be greater than 280, the reduction effect of drag gradually diminishes.

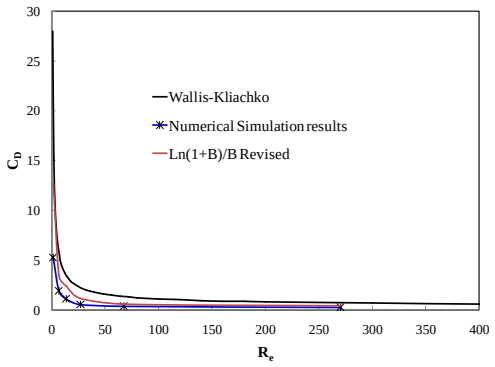

Fig. 9. Drag coefficient vs droplet Reynolds number

Figure 10 shows drag coefficients of droplets of different sizes in their group under various gas relative velocities and temperatures, indicating that the effect of gas temperature is more sensitive to drag reduction.

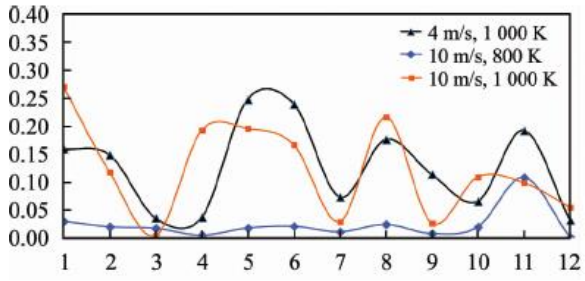

Fig. 10. Drag coefficients of different droplets in their group

Conclusions

Three modes of flame structures were observed in a droplet group: fully-enveloped, partially-enveloped and wake flames, and Stefan-flow structure was observed for the droplet-group combustion, leading to the change of drag force with the increasing inlet velocity. The drag force of combusting multiple droplets is much smaller than that of non-combusting particles in isothermal flows. Future work should be done for finding a new drag-force model of combusting droplets in numerical simulation of spray-combustion engines.

Acknowledgements

This study was sponsored by the Key Project of National Natural Science Foundation of China under the Grant 51390493.

Bibliography

[1] Stelmasiak Z, Matyjasik M. Simulation of the combustion in a dual fuel engine with a divided pilot dose. Combustion Engines, 2012;151(4):43-54. https://doi.org/10.19206/CE-117020

[2] Kniaziewicz T, Zacharewicz M. A physical model of energetic processes in a diesel marine generator set. Combustion Engines. 2018;175(4):10-17. https://doi.org/10.19206/CE-2018-402

[3] Kowalski J. The theoretical investigation on influence the fuel spray geometry on the combustion and emission characteristic of the marine diesel engine. Combustion Engines. 2017;169(2):101-107. https://doi.org/10.19206/CE-2017-218

[4] Li K, Zhou LX, Chan CK, Wang HG. Large-eddy simulation of ethanol spray combustion using a SOM combustion model and its experimental validation. Applied Mathematical Modeling. 2015;39(1):36-49. https://doi.org/10.1016/j.apm.2014.04.011

[5] Li K, Zhou LX. Studies of the effect of spray inlet conditions on the flow and flame structures of ethanol-spray combustion by large-eddy simulation. Numer Heat Transfer, 2012;62(1):44-59. https://doi.org/10.1080/10407782.2012.672865

[6] Godsave GAE. Studies of the combustion of drops in a fuel spray: The burning of single drops of fuel. Symposium (International) on Combustion. 1953;4(1):818-830. https://doi.org/10.1016/S0082-0784(53)80107-4

[7] Spalding DB. The combustion of liquid fuels. Symposium (International) on Combustion. 1953;4(1):847-864. https://doi.org/10.1016/S0082-0784(53)80110-4

[8] Zhou LX. Evaporation and combustion of individual droplets and liquid spray of hydrocarbons in air (in Russian), Ph.D. Thesis, Department of Physics and Mechanics, Leningrad Polytechnic University, USSR, 1961.

[9] Law CK. Recent advances in droplet vaporization and combustion. Prog Energ Combust. 1982;8(3):171-201. https://doi.org/10.1016/0360-1285(82)90011-9

[10] Awasthi I, Pope DN, Gogos G. Effects of the ambient temperature and initial diameter in droplet combustion. Combust Flame. 2014;161(7):1883-1899. https://doi.org/10.1016/j.combustflame.2014.01.001

[11] Kitano T, Nishio J, Kurose R, Komori S. Effects of ambient pressure, gas temperature and combustion reaction on droplet evaporation, Combust Flame. 2014;161(2):551-564. https://doi.org/10.1016/j.combustflame.2013.09.009

[12] Zhao Y, Yang LB, et al. Numerical simulation of impacts of gas flow temperature on combustion characteristics of single droplet. Journal of Combustion Science and Technology (in Chinese). 2014;20:77-83.

[13] Tsai HL, Chiu HH. Anomalous group combustion phenomena in DI diesel engines. Atomization Sprays. 2005;15:377-400. https://doi.org/10.1615/AtomizSpr.v15.i4.20

[14] Tsai HL, Chiu HH. Cluster statistical theory based on group combustion, 4th Asia-Pacific Conference on Combustion. 2003:491-494.

[15] Segawa D, Yoshida M, Nakaya S, Katoda T. Auto-ignition and early flame behavior of a spherical cluster of 49 monodispersed droplets. P Combust Inst. 2007;31(2):2149-2156. https://doi.org/10.1016/j.proci.2006.07.124

[16] Mikami M, Matsumoto K, Yoshida Y, Kikuchi M, Dietrich DL. Space-based microgravity experiments on flame spread over randomly distributed n-decane droplet clouds: anomalous behavior in flame spread. P Combust Inst. 2021;38(2):3167-3174. https://doi.org/10.1016/j.proci.2020.07.139

[17] Mikami M, Yoshida Y, Seo T, Sakashita T, Kikuchi M, Suzuki T et al. Space-based microgravity experiments on flame spread over randomly distributed n-decane droplet clouds: overall flame spread characteristics. Microgravity Sci Tech. 2018;30:535-542. https://doi.org/10.1007/s12217-018-9637-2

[18] Manish M, Sahu S. Optical characterization of droplet clusters and group combustion in spray diffusion flames. P Combust Inst. 2021;38(2):3409-3416. https://doi.org/10.1016/j.proci.2020.08.016

[19] Eisenklam P, Arunachalam SA. The drag resistance of burning drops. Combust Flame. 1966;10(2):171-176. https://doi.org/10.1016/0010-2180(66)90065-4

[20] Yuen MC, Chen LW. On drag of evaporating liquid droplets. Combust Sci Technol. 1976;14(4-6):147-154. https://doi.org/10.1080/00102207608547524

[21] Renksizbulut M, Yuen MC. Numerical study of droplet evaporation in a high-temperature stream. J Heat Transf. 1983;105(2):389-397. https://doi.org/10.1115/1.3245591

[22] Makino A, Fukada H. Combustion behavior of a falling sodium droplet: burning rate and drag coefficient. Heat Transfer-Asian Research. 2005;34(7):481-495. https://doi.org/10.1002/htj.20084

[23] Sugimoto A. Investigation of combustion of liquid sprays II: drag coefficient of a droplet. Bulletin of University of Osaka Prefecture, Series A. 1970;19:35-44.

[24] Germano M, Piomelli U, Moin P, Cabot WH. A dynamic subgrid-scale eddy viscosity model. Phys Fluids A-Fluid. 1991;3:1760-1765. https://doi.org/10.1063/1.857955
[25] Zhou L. Development of SOM combustion model for Reynolds-averaged and large-eddy simulation of turbulent combustion and its validation by DNS. Sci China Ser E-Technol Sci. 2008;51:1073-1086. https://doi.org/10.1007/s11431-008-0157-y
[26] Zhou L, Li K. Analytical and numerical studies on a single-droplet evaporation and combustion under forced convection. Acta Mech Sin. 2015;31:523-530. https://doi.org/10.1007/s10409-015-0424-7
[27] Mercier X, Orain M, Grisch F. Investigation of droplet combustion in strained counterflow diffusion flames using planar laser-induced fluorescence. Appl. Phys B. 2007;88: 151-160. https://doi.org/10.1007/s00340-007-2605-y
[28] Zhou L. Combustion Theory and Dynamics of Reacting Fluids. Beijing: Science Press; 1986.

Prof. Lixing Zhou, DSc., DEng. – Engineering Mechanics, Tsinghua University, China.
e-mail: *zhoulx@mail.tsinghua.edu.cn*

Prof. Ke Li, DSc., DEng. – School of Energy and Environmental Engineering, Inner Mongolia University of Science and Technology, China.
e-mail: *kelitsinghua@hotmail.com*

Ting Sun, DEng. – Engineering Mechanics, Tsinghua University, China.
e-mail: *sunting@imust.edu.cn*